New Folder Name Proposal for Recombination

Proposal for Recombination of the 40-m Interferometer

Torrey Lyons and Fred Raab

October 6, 1994

Abstract

A proposal to recombine the 40-m interferometer is presented.

1 Introduction

The initial interferometer design chosen for LIGO is an asymmetric power recycled Michelson with Fabry-Perot cavities as shown in Figure 1.[1] Four degrees of freedom need to be controlled. These are the recycling cavity length ($l_1 + l_2$), the Michelson near-mirror difference ($l_1 - l_2$), the common mode arm cavity length ($L_1 + L_2$), and the arm cavity length difference ($L_1 - L_2$) which gives the gravitational wave signal. Two schemes for extracting signals proportional to the auxiliary degrees of freedom will be evaluated.*

Figure 1 Asymmetric Power Recycled Michelson with Fabry-Perot Cavities

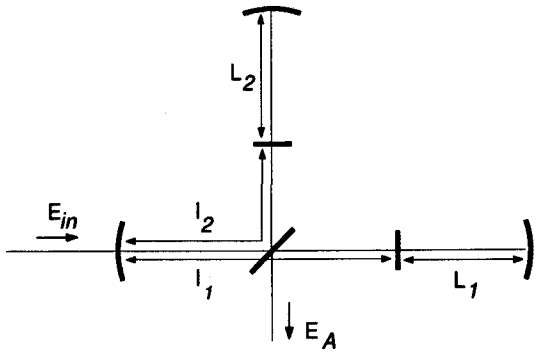

Eventually the 40-m interferometer must include the complete LIGO optical topology with both signal extraction schemes. What is described here is a plan to move towards this goal in steps. In particular, a detailed proposal is given

* Auxiliary degrees of freedom are all the degrees of freedom except for the arm cavity length difference which provides the gravitational wave signal.

to change the 40-m interferometer to a recombined optical topology using the asymmetry signal extraction scheme within the next 6–8 months. Following this work it is expected that the frequency shifted subcarrier signal extraction scheme and ultimately a full recycled optical topology will be implemented. This future work would have to be scheduled in concert with other 40-m interferometer activities. We believe, however, that there is currently a window of opportunity to finish the recombination task without significantly displacing other work.

A diagram of the recombined optical topology with asymmetry scheme signal extraction is shown in Figure 2. The beam splitter and arm cavity mirrors are labelled as mirrors 2 through 6.† For a non-recycled interferometer the $l_1 + l_2$ degree of freedom is not important. The asymmetry is the DC value of $l_1 - l_2$.‡ The three extracted signals are v_1, v_2, and v_3. The signal v_1 is used to control the common mode arm cavity length and is fed back to the laser frequency servo. The signal v_2 is fed back to control the beam splitter position. And, the signal v_3 is used to control the differential arm cavity length.

Figure 2 Recombined Optical Topology and Extracted Signals

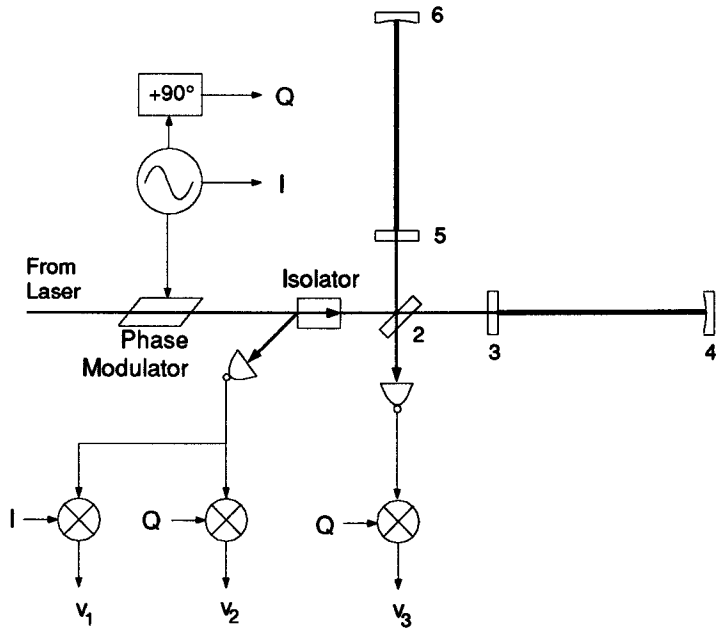

† This is to maintain the same numbering convention as earlier papers on recycling/recombination where the recycling mirror would be mirror 1.

‡ In a non-recycled interferometer these lengths are defined relative to the beam splitter instead of the recycling mirror.

Each extracted signal depends mostly on the degree of freedom it controls. The cross coupling to other degrees of freedom is of order 10^{-4} for all the extracted signals.* Because the three servo loops are largely independent we should be able to acquire lock with the asymmetry scheme without the need for a frequency shifted subcarrier. The advantage to proceeding first to the asymmetry scheme is that it will be easier to implement.

The attraction of implementing recombination seperately from recycling is that it forms a managable, closed-ended project which will yield valuable information for recycling. In particular, recombination would provide information on contrast defect, intensity noise, frequency noise, and asymmetry signal extraction control systems. In fact the methods of signal extraction and the feedback loop shapes (up to an overall constant gain factor) used for recombination will be almost identical to those for recycling except for the exclusion of the recycling mirror loop. Most of the work that is planned for the recombination task is necessary to implement recycling. Recombination also has the potential to improve the shot noise limited sensitivity by allowing the incident laser power to be increased without saturating the RF photodiodes. A modest improvement in shot noise limited sensitivity per unit laser power could also be achieved fairly easily by increasing the RF modulation frequency to 37 MHz.

Recombination in the 40-m interferometer could begin within two months which is the approximate time frame for completion of the monolithic test mass task and time domain data analysis runs. The work in the 40-m lab would proceed roughly as follows.†

- Move test masses to provide a 50 cm asymmetry. (1 month)
- Check system integrity by running in old servo configuration. (1 week)
- Remove circulators and demonstrate locking in new configuration. (2 — 4 weeks)
- Achieve and understand a stable noise spectrum comparable to current noise. (2 — 4 months)

We believe that lock acquisition is the largest uncertainty in this process.

All of the points raised above are discussed in more detail in the following sections. In Section 2 we describe the technical issues involved in exploring

* This was not true in Martin's recycled asymmetry scheme prototype, where the signal controlling the recycling mirror position was very ill-conditioned. In addition the higher finesse arm cavities in the 40-m interferometer greatly improve the condition of the other signals. This is discussed in more detail in Section 2.

† A more detailed schedule is given in Section 3.

the feasibility of recombination. Section 3 presents a draft schedule of the recombination task. In Section 4 the ramifications of recombination on the future task of recycling is considered. And in Section 5 we present our conclusions.

2 Technical Issues

For a recombined interferometer there are three degrees of freedom which need to be controlled. For the following discussion we shall consider these distances in units of round-trip phase at the laser frequency. That is,

$$\phi_- = \frac{4\pi}{\lambda}(l_1 - l_2) \qquad \Phi_- = \frac{4\pi}{\lambda}(L_1 - L_2) \qquad \Phi_+ = \frac{4\pi}{\lambda}(L_1 + L_2) \qquad (1)$$

modulo 2π. The resonance conditions for these degrees of freedom are that they equal zero.[‡]

The parameters used in the calculations below for the initial recombination of the 40-m interferometer are shown in Table 1. The losses quoted are measured from the east arm and split evenly between the mirrors.[§] South arm losses are comparable. (Both arms appear to have a much higher loss that was expected from ringdowns of individual test masses in the optics lab.) The arm cavity input couplers have 4 — 9 ppm transmission peaks in their centers with FWHM of 5 mm. The transmission values given are for the central peak transmission.

Table 1 Parameters for 40-m Interferometer Recombination

Quantity	Symbol	Value
Mirror (power) transmissions	T_2	0.45
	T_3	281 ppm
	T_5	261 ppm
	T_4, T_6	12 ppm
Loss in each mirror	L	96 ppm
Asymmetry	δ	50 cm (nominal)

‡ Strictly speaking there is no resonance associated with $\phi_- = 0$, but we will use the term to indicate that this is the optimal operating point of the interferometer.

§ For a high finesse Fabry-Perot cavity it does not matter much where the losses are distributed.

Table 1 (Continued) Parameters for 40-m Interferometer Recombination

Quantity	Symbol	Value
Modulation frequency	f_{mod}	12.33 MHz
Modulation index	Γ	0.84 (optimal)
Contrast Defect	$1 - C$	0.01

For a laser interferometer with Fabry-Perot arms the definition of contrast is somewhat ambiguous. The definition we shall use here is:

$$C \equiv \frac{P_B - P_D}{P_B + P_D} \tag{2}$$

where P_B and P_D are the maximum and minimum powers measured at the antisymmetric port. P_B will be measured when both arm cavities are off resonance and there is constructive interference at the antisymmetric port,[‖] while P_D will be measured when both arm cavities are on resonance and there is destructive interference at the antisymmetric port.

The relative sensitivities of the signals to changes in the three degrees of freedom is shown in Table 2 in arbitrary units, normalized so that the gravitational wave readout sensitivity is one.[#] Thus, for example,

$$\frac{\partial v_1}{\partial \Phi_+} = 6.40224. \tag{3}$$

Notice that the sensitivity to arm cavity common mode motion is higher than the sensitivity to differential motion. This is because the small 50 cm asymmetry provides poor transmission of the RF sidebands to the asymmetric port and good transmission to the symmetric port.[**]

Table 2 Extracted Signal Sensitivities

	∂v_1	∂v_2	∂v_3
$\partial \Phi_+$	6.40224	0	0
$\partial \phi_-$	0	6.82652×10^{-5}	6.82652×10^{-5}
$\partial \Phi_-$	0	5.12086×10^{-9}	1.00000

‖ Effectively, P_B equals the incident power. One could also define P_B to be with the arm cavities held on resonance. In this case P_B would equal the incident power times the arm cavity visibility.

\# The table was computed by a Mathematica program written by Martin Regehr.

** This will improve when the interferometer is recycled later.

The issues considered in exploring the feasibility of recombination of 40-m interferometer are discussed in detail below. They are:

- Shot noise in the gravitational wave signal
- Shot noise in the arm cavity common mode signal
- Shot noise in the beam splitter position signal
- Residual RMS arm cavity difference motion
- Residual RMS arm cavity common mode motion
- Residual RMS beam splitter motion
- Output noise in the beam splitter coil driver
- Mixer phase error
- Contrast Defect
- Intensity Noise

None of these issues present a significant difficulty.

Issues Considered

Shot noise in the gravitational wave signal The predicted shot noise limited sensitivity of the 40-m interferometer using the current optical topology[2] and with a recombined topology[3] are shown in Figure 3 for 150 mW of light incident on the beam splitter. Because of the small asymmetry there is a degradation in sensitivity with recombination, but it is only –1.1 db. The recombined optical topology allows a much higher incident power without problems with saturation of the RF photodiodes. Thus an increase in incident power could offset the degradation in shot noise. Once the recombination task is completed the modulation frequency could be fairly easily upgraded to 37 MHz. The sensitivity for the interferometer in this configuration is also shown in Figure 3.

Figure 3 Shot Noise Limited Sensitivity

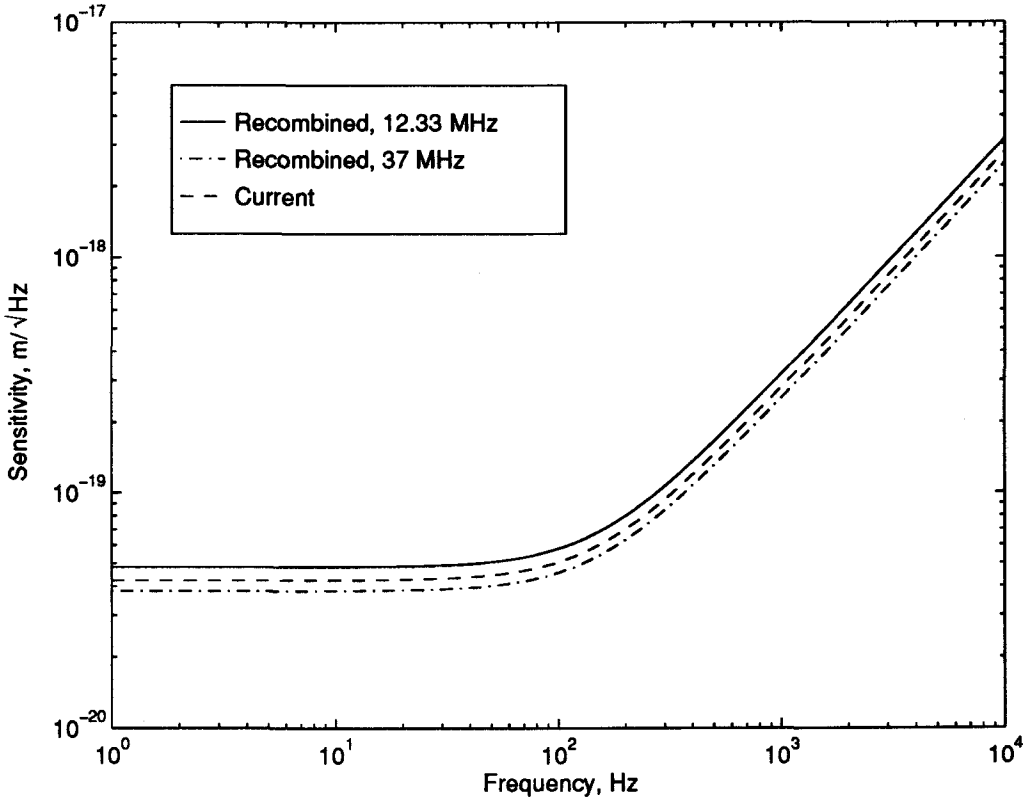

Shot noise in the arm cavity common mode signal The shot noise limited sensitivity to arm cavity common mode motion will have the same frequency dependence as the shot noise limited sensitivity to differential motion.[††] We can approximate the ratio between the DC sensitivities to common mode and differential motion by scaling by the powers falling on the two detectors and the sensitivity of each detector to phase variation in the sensed degree of freedom. P_S is the power of the light returning to the laser which is deflected by the optical isolator and P_A is the power of the light exiting the antisymmetric port. We also define η_S and η_A as the quantum efficiencies of the corresponding photodiodes. These

[††] That is a single pole at the cavity corner frequency as shown in Figure 3 for the differential motion.

quantum efficiencies include the effects of attenuators placed before the photodiodes. The signal sensing the Φ_+ degree of freedom is proportional to $\eta_S \frac{\partial v_1}{\partial \Phi_+}$. The noise is proportional to $(\eta_S P_S)^{\frac{1}{2}}$. Using the analogous relations for Φ_- we get

$$\left(\frac{S_{\Phi_+}(0)}{S_{\Phi_-}(0)}\right)^{\frac{1}{2}} \approx \left(\frac{P_S}{P_A}\right)^{\frac{1}{2}} \left(\frac{\eta_A}{\eta_S}\right)^{\frac{1}{2}} \frac{\frac{\partial v_3}{\partial \Phi_-}}{\frac{\partial v_1}{\partial \Phi_+}} \tag{4}$$

where $S^{\frac{1}{2}}_{\Phi_+}$ is the shot noise limited sensitivity to the Φ_+ degree of freedom and similiarly for $S^{\frac{1}{2}}_{\Phi_-}$.

Currently we achieve arm cavity visibilities of approximately 60%. Thus we expect about 40% of the incident light to return to the symmetric port. Optimal modulation depth corresponds to having roughly as much light from the sidebands at the antisymmetric port as carrier due to contrast defect. Thus the power at the antisymmetric port is approximately 1% of the incident light and

$$\frac{P_S}{P_A} \approx 40. \tag{5}$$

When operating the interferometer at full power, both signal extraction photodiodes will need to have some kind of bright fringe protection for the out of lock state. Developing this bright fringe protection is beyond the scope of the initial recombination task, but we can safely run at current power levels without it.

Once in lock the symmetric port light will have to be attenuated when running at full power. The current RF photodiodes have only been operated with a power of slightly over 50 mW. The largest reasonable amount of incident laser power is 1 W. Thus, in our in lock state we expect

$$1.0 < \frac{\eta_A}{\eta_S} < 8.0 \tag{6}$$

depending on the incident power. Using the signal sensitivities in Table 2 and the worst case estimate from eq. (6) we calculate,

$$\left(\frac{S_{\Phi_+}(0)}{S_{\Phi_-}(0)}\right)^{\frac{1}{2}} \approx 2.8. \tag{7}$$

This should be adequate for control of the arm cavity common mode length.

Shot noise in the beam splitter position signal The shot noise limited sensitivity to beam splitter position is flat with frequency. We can approximate the desired shot noise ratio by using the same scaling law used for shot noise in the arm cavity common mode signal.

$$\left(\frac{S_{\phi\_}(0)}{S_{\Phi\_}(0)}\right)^{\frac{1}{2}} \approx \left(\frac{P_S}{P_A}\right)^{\frac{1}{2}} \left(\frac{\eta_A}{\eta_S}\right)^{\frac{1}{2}} \frac{\frac{\partial v_3}{\partial \Phi\_}}{\frac{\partial v_2}{\partial \phi\_}} \tag{8}$$

Using our previous estimates for light powers and quantum efficiencies we find,

$$\left(\frac{S_{\phi\_}(0)}{S_{\Phi\_}(0)}\right)^{\frac{1}{2}} \approx 2.6 \times 10^5. \tag{9}$$

This level of shot noise will not limit gravitational wave sensitivity. This is discussed in Appendix B.

Residual RMS arm cavity difference motion The arm cavity difference is analogous to the current second arm length. The sensitivity to motion in this degree of freedom is approximately the same as the current system's sensitivity to second arm length. The coil-driven magnet actuators used in both cases are identical. Thus we expect that by using the existing second arm control system we can achieve a limit on RMS arm cavity difference very nearly the same as is achieved currently for the second arm length. The current second arm servo can supress length variations to 8×10^{-14} m RMS.[4] As shown in Appendix A, the performance requirement for arm cavity difference is that the RMS motion must be $< 1 \times 10^{-13}$ m. Thus the current second arm control system should be adequate for controlling the arm cavity difference.

Residual RMS arm cavity common mode motion This degree of freedom is analagous to the current first arm length. As discussed for the RMS arm cavity difference, we expect to be able to achieve performance similiar to that achieved in the current first arm loop, because the sensitivities and the methods of actuating control signals are very similiar in both cases. The RMS motion of the first arm is least as small as the second arm because the loop gain is much higher. In Appendix A a performance requirement on RMS arm cavity common mode motion of $< 6 \times 10^{-12}$ m is given. Therefore we expect the current first arm control system to be adequate for controlling the arm cavity common mode length.

Residual RMS beam splitter motion Seismic noise in the beam splitter position must not degrade the dark fringe at the antisymmetric port. In Appendix B it is concluded that the beam splitter can be controlled to meet this requirement.

Output noise in the beam splitter coil driver From Table 2 it can be seen that the gravitational wave signal, v_3, is sensitive to a small degree to motions of the beam splitter. If the output noise of the beam splitter coil driver in the gravitational wave band is too high, this could corrupt the gravitational wave readout. It is shown below that this will not limit the gravitational wave sensitivity at frequencies down to at least 100 Hz.

Seiji has measured the output noise at 100 Hz to be 30 $\mathrm{nV}/\sqrt{\mathrm{Hz}}$.[5] The conversion to actual displacement has been measured to be on the order of 1 mm/V at DC.[6] Thus, accounting for the pendulum suspension, at 100 Hz the output noise is

$$S_o^{\frac{1}{2}} \sim 3 \times 10^{-15}\ \mathrm{m}. \tag{10}$$

The arm cavity difference motion equivalent to this beam splitter motion in the gravitational wave signal is

$$\begin{aligned} S_{arm}^{\frac{1}{2}} &= \frac{\frac{\partial v_3}{\partial \phi_-}}{\frac{\partial v_3}{\partial \Phi_-}} S_o^{\frac{1}{2}} \\ &\sim 2 \times 10^{-19}\ \mathrm{m}/\sqrt{\mathrm{Hz}}. \end{aligned} \tag{11}$$

Mixer phase error An error in the phase of the local oscillator used to demodulate the symmetric port signal and generate v_2 will allow some of the v_1 signal to leak into the beam splitter control loop. This is a problem because v_2 is fairly insensitive to beam splitter motion. The amount of phase error that can be tolerated depends on the degree to which the frequency stability servo can suppress error in the arm cavity common mode length. For a residual RMS error of 10^{-13} m in the arm cavity common mode, a 5° mixer phase error will cause v_2 to have a contribution from arm cavity common mode length to be 1/4 the contribution from beam splitter position. Mixer phase has been measured to drift approximately 1° over hours with occasional excursions of 2° on several minute timescales. Thus with careful initial adjustment, mixer phase error should not be a problem.

In the presence of mixer phase error the signal at v_2 is:[7]

$$v_2 \propto \frac{\partial v_2}{\partial \phi_-} e_2 + \frac{\partial v_1}{\partial \Phi_+} \sin\beta \, e_1 \tag{12}$$

where e_2 is the error in the beam splitter position, e_1 is the error in the arm cavity common mode length, and β is the mixer phase error. The ratio of the importance of e_2 and e_1 in v_2 is

$$K = \frac{\frac{\partial v_1}{\partial \Phi_+}}{\frac{\partial v_2}{\partial \phi_-}} \sin\beta. \tag{13}$$

An arm cavity common mode RMS error, $e_1 = 10^{-13}$ m is achievable. For $\beta = 5°$, $K = 8200$ so that the contribution of v_2 from e_1 is equivalent to 8.2×10^{-10} m of beam splitter motion. As discussed in Appendix B the residual RMS beam splitter motion is estimated to be on the order of 3×10^{-9} m. Thus the beam splitter contribution is approximately a factor of four larger for this mixer phase error.

Contrast Defect We have specified a target contrast defect of 1%. This number was chosen because we believe it is achievable, it gives reasonable shot noise limited sensitivity, and it close to the specification being set for LIGO. There are three mechanisms we have considered for contrast defect. These are wavefront distortion due to arm cavity mirror imperfections, different visibilties in the two arms, and pointing errors in the beams returning from the arms.

We expect that wavefront distortions will not degrade the contrast beyond 1%. In a table top demonstration of recycling using the asymmetry signal extraction scheme a 1% contrast defect was seen with 6 m long, folded arm cavities.[8]

If the arms cavities have different visibilities, the difference in the amount of light returning from each arm will cause a contrast defect.

$$1 - C \simeq 2\frac{P_A}{P_{in}} = \left|\sqrt{1 - V_1} - \sqrt{1 - V_2}\right|^2 \tag{14}$$

where P_A is the power at the antisymmetric port, P_{in} is the incident power, and V_1 and V_2 are the visibilities of the two arms with zero modulation depth.* The cavity visibility is defined as

$$V = \frac{P_{max} - P_{min}}{P_{max}} \tag{15}$$

* The phase modulation will decrease the arm cavity visibilities. Contrast defect is defined for power in the carrier so it is the zero modulation depth limit which is important here.

where P_{max} is the maximum power (out of lock) that returns from the cavity, and P_{min} is the minimum (in lock) power that returns. A visibility difference could occur due to unbalanced losses in the two arms or alignment errors. With the mirror parameters given in Table 1 the maximum arm cavity visibilities without modulation are 97.5% and 98.5%. The maximum visibilites actually achieved in the 40-m interferometer have consistently been about 92% of the theoretical maximum due to mode matching errors.[9] Thus we expect to achieve visibilites without modulation of 89.7% and 90.6%.* These visibilities correspond to a contrast defect of 0.02%. A 7% drop in visibility in one arm would lead to a 0.9% contrast defect. Such a visibility drop would correspond to roughly a 300 ppm total increase in cavity losses. Typical visibility fluctuations due to mirror alignment errors are smaller than this. Thus we do not expect visibility differences to degrade the contrast defect beyond 1%.

An angular tilt of the beam axis for the beam returning from one arm will cause imperfect interference at the beam splitter. This could be caused by mirror orientation noise. An angular tilt α will cause the phase fronts of the interfering beams from the two arms to no longer be parallel and the spot positions to be shifted relative to each other. The fraction of the power which does not interfere destructively at the antisymmetric port due to the non-parallel phase fronts is

$$k_1 = \left(\frac{\alpha \pi w}{\lambda}\right)^2 \tag{16}$$

where w is the beam waist (radius).[10] The fraction due to spot position movement is

$$k_2 = \left(\frac{l\alpha}{w}\right)^2 \tag{17}$$

where l is the distance between the input test mass and the beam splitter. In the 40-m interferometer $l \approx 2$ m. As a worst case estimate for the angular tilt in the returning beam axis we use the orientation noise of the test masses. Thus, $\alpha \approx 5 \times 10^{-6}$ rad, or 0.2 mm over 40 m. So $k_1 = 0.45$ % and $k_2 = 0.002$ %. The contrast defect from this is given by

$$\begin{aligned} 1 - C &= 2\,(1 - V)\,(k_1 + k_2) \\ &= 0.09\,\% \end{aligned} \tag{18}$$

Thus this effect is negligible.

* The visibilities actually achieved are around 60% due to the modulation.

Intensity Noise The asymmetry used in the signal extraction scheme may make the interferometer more sensitive to laser intensity noise. A generally accepted model of this effect does not currently exist, but a recombined optical topology will provide experimental verification for whichever model is adopted. The recombined topology in particular is sensitive to this effect as it does not benefit from the filtering effect of the recycling cavity.

3 Draft Schedule

Preparation (2 months)

Parts Needed

1. Vacuum compatible 1.5″ mirrors and mounts — total of 5
   a. Antisymmetric recombined beam (already installed)
   b. Symmetric recombined beam — 3
   c. EV local pointing beams — 2
2. Vacuum compatible Faraday isolator
3. Periscopes — 2 (in house)
4. Steering mirrors and mounts — 4 (in house)
5. Beam splitter (BS) servo amplifier
6. Coil driver decoder with sum and difference inputs

Work

1. Steer antisymmetric recombined beam out of vacuum envelop during next vent. (done)
2. Restore DC drive capability to translation stage of BS OSEM controller. (1 day)
3. Have new drawings made of inside of BS and test mass chambers. (1 week)
4. Plan layout for exterior signal extraction photodiodes. (1/2 day)

Implementation (4 — 6 months)

1. Vent and move east arm masses away from BS by 25 cm and south arm test masses closer to BS by 25 cm. Install Faraday isolator and symmetric recombined beam steering mirrors in BS chamber. (1 month)

2. Pump down and demonstrate identical noise performance in old optical topology with new test mass locations. (1 week)
3. Vent and remove circulators. (1 week)
4. Wire electronics for recombined servo control. (1/2 week)
5. Pump down, acquire lock and take a displacement spectrum. (1 — 3 weeks)
6. Shakedown. This includes achieving a displacement sensitivity comparable to the current 40-m spectrum and understanding the noise sources limiting the sensitivity in the recombined configuration. (2 — 4 months)

4 Ramifications for Recycling

The primary reason for the recombination of the 40-m interferometer is that it furthers the effort to move the 40-m interferometer to a full recycled configuration. This section will discuss what we expect to learn from recombination and how the physical modifications to the interferometer affect recycling.

The choice of arm cavity input mirrors for recycling will be aided by knowledge of the contrast defect we achieve. A recombined topology gives us the option of installing input mirrors suitable for recycled operation before installing a recycling mirror. This would be very difficult with the current configuration. In this way we could select the optimal recycling mirror transmission to order.

Recombination would also serve as a test bed for the control of three degrees of freedom using hanging mirrors. The exact servo topology to be used with the asymmetry signal extraction scheme has not been selected, but in two of the three configurations considered the beam splitter is controlled as we have proposed.[†11] The loop shapes used for recombination should be identical to those needed for recycling except for the effect of moving the arm cavity pole in the Φ_- and Φ_+ loops and the addition of the recycling cavity pole in the ϕ_- loop. All of these changes should not significantly change the electronics and are easily modelled using modern control theory. The recombined 40–m interferometer will also allow significant testing of signals associated with the single sideband modulation technique without the added complexity associated with the introduction of the recycling mirror.

† The configuration considered in the body of Martin Regehr's Ph.D. thesis involves feedback to all four arm cavity mirrors instead of the beam splitter. In this way one arm is driven closer to the beam splitter while the other is driven away to control ϕ_-. This configuration is probably more tractable mathematically, but appears less appealing for practical implementaion.

Moving test masses to provide an asymmetry for signal extraction accomplishes the largest and most delicate modification to the interferometer which is necessary for recycling. The 50 cm value chosen for the asymmetry is the maximum which the current vacuum chambers and test masses suspensions can easily accomodate. For a recycled interferometer the optimal asymmetry is given by[12]

$$\begin{aligned} \cos\alpha &= r_R\, T_p \\ \alpha &= \frac{\delta\Omega}{c} \end{aligned} \tag{19}$$

where Ω is the angular modulation frequency, r_R is the recycling mirror reflectivity and T_p is the transmission of the recycling cavity pickoff. The recycling factor for the 40-m interferometer will probably be around 5. With this recycling factor the optimal asymmetry in units of phase is $\alpha \approx 0.48$. For 12.33 MHz modulation this corresponds to an asymmetry of $\delta \approx 1.9$ m while for 37 MHz modulation the optimal asymmetry is 62 cm. Avoiding gain constraints on the loops controlling ϕ_+ and Φ_+ requires[13]

$$\cos\alpha > r_{arm} \tag{20}$$

where r_{arm} is the amplitude reflectivity of the arm cavities. For a recycling factor of 5 this corresponds to the constraint $\alpha < 0.46$. For 12.33 MHz modulation this requires $\delta < 1.8$ m and for 37 MHz modulation $\delta < 60$ cm. Thus a 50 cm asymmetry will be adequate for recycling with a recycling factor of 5. If higher recycling factors are desired then a tradeoff between modulation frequency and asymmetry must be made. For example with a reycling factor of 10 the asymmetry limit for 37 MHz modulation is $\delta < 41$ cm.

5 Conclusion

We believe that the opportunity exists at the present time to gain important knowledge and make progress towards recycling without seriously disrupting other 40-m priorities. Because the idea of recombination before recycling had not previously been given much serious thought, a rather involved treatment of the technical issues has been presented. This treatment shows that a recombined 40-m interferometer is feasible and would operate with noise performance similiar to or better than the current prototype.

Appendix A Allowable Residual RMS Deviations[14]

This appendix gives reasonable specifications on the allowable RMS deviations from resonance for the three degrees of freedom which will guarantee adequate gravitational wave sensitivity. Deviations from resonance can degrade the interferometer performance in several ways. The specifications given below are based on the need to maintain adequate power in the arm cavities, reject laser frequency or intensity noise, and keep the antisymmetric port dark.

A deviation from resonance of the common mode arm cavity length will cause the power in the arm cavities to drop, decreasing the gravitational wave signal. We take the specification that the power in the arms must stay within 90% of the maximum. For a single arm cavity to maintain the power at 90% of maximum requires that the phase deviation from resonance, $\delta\phi$, satisfies[15]

$$\delta\phi < 0.3\,\frac{1 - r_3 r_4}{r_3 r_4}. \tag{21}$$

If we consider displacing both arm cavities from resonance equally then the specification on the common mode length is

$$\begin{aligned} \Phi_+^{rms} &< 0.6\,\frac{1 - r_3 r_4}{r_3 r_4} \\ &< 1.5 \times 10^{-4}. \end{aligned} \tag{22}$$

In more familiar units this corresponds to an RMS deviation of 6×10^{-12} m.

The gravitational wave signal is proportional to the product of the laser power and the arm cavity length difference. Thus, low frequency deviations from resonance in Φ_- can cause laser intensity noise in the gravitational wave band to corrupt the gravitational wave signal. Currently about 5 mW is picked off to power stabilize the laser. Assuming the intensity noise is shot noise limited, the relative intensity noise is

$$\begin{aligned} \frac{S_I^{\frac{1}{2}}(f)}{I} &= \sqrt{\frac{2h\nu}{\eta P}} \\ &= 1.4 \times 10^{-8}/\sqrt{Hz} \end{aligned} \tag{23}$$

where ν is the laser frequency, η is the quantum efficiency of the detector (assumed to be 80%), and P is the power picked off for power stabilization. The contribution

of the gravitational wave signal from intensity noise should be smaller than the contribution from arm cavity difference. Thus,

$$\begin{aligned} \Phi_-^{rms} \frac{S_I^{\frac{1}{2}}(f)}{I} I &< S_{\Phi\_}^{\frac{1}{2}}(f)\, I \\ \Phi_-^{rms} &< \left(\frac{S_I^{\frac{1}{2}}(f)}{I} \right)^{-1} S_{\Phi\_}^{\frac{1}{2}}(f) \end{aligned} \tag{24}$$

where $S_{\Phi\_}^{\frac{1}{2}}(f)$ is the desired sensitivity to the arm cavity difference. A target best sensitivity of $10^{-19}\,\mathrm{m}/\sqrt{\mathrm{Hz}}$ corresponds to $S_{\Phi\_}^{\frac{1}{2}}(f) = 2.4 \times 10^{-12}/\sqrt{\mathrm{Hz}}$. Thus we require,

$$\Phi_-^{rms} < 1.7 \times 10^{-4} \tag{25}$$

which corresponds to 7×10^{-12} m.

A recombined interferometer will reject frequency noise to some extent. If the arm cavities have the same storage time and are both on resonance, changing the laser frequency will cause the phase of the light reflected from both arms to rotate by the same amount. Thus the effect will cancel out and no signal will be seen upon recombination at the beam splitter. Various imperfections degrade this frequency noise rejection, nonetheless a recombined interferometer will certainly provide more rejection than the current 40-m interferomter which has none. We expect that the mismatch in arm cavity storage times with the current mirrors will be the primary limitation to achieving good frequency noise rejection. In particular to meet the LIGO specification of 99% frequency noise rejection requires matching the storage times to better than one part in 100.[16,17] If the arm cavities are sufficiently well matched then we must satisfy

$$\Phi_+^{rms}\Phi_-^{rms} < 2 \times 10^{-6} \tag{26}$$

to hold the arms cavities sufficiently close to resonance.[18] If Φ_+^{rms} just satisfies the condition above, then we require

$$\Phi_-^{rms} < 1.3 \times 10^{-2}. \tag{27}$$

This condition is much weaker than the condition from intensity noise. Thus laser frequency noise rejection will not be limited by deviations from resonance, but more likely because of arm cavity loss mismatches.

Deviations from resonance in ϕ_- or Φ_- degrade the dark fringe at the antisymmetric port and thereby increase the shot noise in the gravitational wave signal. As discussed previously the contrast defect has been specified to be 1%. We adopt the criteria that no more than an additional 0.2% of the incident power go to the antisymmetric port due to motion of the beam splitter and similiarly for arm cavity differential motion. With the arm cavities in perfect resonance, assuming negligible losses in all the optical elements, the power transmission from the laser input beam to the antisymmetric port is $\sin^2\left(\frac{\phi_-}{2}\right)$. Thus we require,

$$\begin{aligned} \sin^2\left(\frac{\phi_-^{rms}}{2}\right) &< 0.002 \\ \phi_-^{rms} &< 8.9 \times 10^{-2} \end{aligned} \tag{28}$$

or that the RMS Michelson near mirror difference $< 4 \times 10^{-9}$ m.

To derive the analogous specification for the arm cavity length difference we note that the phase of the light returning to the beam splitter changes much faster for changes in Φ_- than for changes in ϕ_-. The exact ratio of this rate of change of phase is the so-called "augmented bounce number".[19] On resonance it is given by

$$\begin{aligned} N' &= \frac{-T_3 r_4}{(r_3 - (1 - L_3)r_4)(1 - r_3 r_4)} \\ &= 30,200. \end{aligned} \tag{29}$$

Thus the specification for Φ_- must be tighter by this factor so that

$$\Phi_-^{rms} < 2.9 \times 10^{-6}. \tag{30}$$

This corresponds to an RMS arm cavity length difference of 1×10^{-13} m.

We adopt as our specification the strictest criteria for each of the three degrees of freedom. The final specifications are summarized in Table 3.

Table 3 Specifications for RMS Deviations

Phase	Distance, m	Explanation
$\Phi_+ < 1.5 \times 10^{-4}$	$L_1 + L_2 < 6 \times 10^{-12}$	arm cavity power
$\phi_- < 8.9 \times 10^{-2}$	$l_1 - l_2 < 4 \times 10^{-9}$	maintain dark fringe
$\Phi_- < 2.9 \times 10^{-6}$	$L_1 - L_2 < 1 \times 10^{-13}$	maintain dark fringe

Appendix B Shot Noise in the Beam Splitter Control Loop

As we can see from Table 2, the gravitational wave output, v_3, is not only sensitive to differential arm cavity motion but also to beam splitter motion. If the beam splitter is moving at frequencies in the gravitational wave band this may corrupt the gravitational wave signal. This is potentially a problem because the sensing of the beam splitter position is fairly noisy due to shot noise.

Quantitatively, we require that above 100 Hz the gravitational wave sensitivity limit due to beam splitter motion is less than the limit due to shot noise at the antisymmetric port. At these frequencies the beam splitter control loop sensors will be dominated by shot noise and will impress this noise multiplied by the complementary sensitivity, T, upon the beam splitter position. The complementary sensitivity is defined as

$$T = \frac{G}{1+G} \tag{31}$$

where G is the open loop gain in the beam splitter control loop. Thus we require that for $f \geq 100\ Hz$

$$\begin{aligned} S^{\frac{1}{2}}_{\phi\_}(f)\, T(f)\, \frac{\partial v_3}{\partial \phi\_} &< S^{\frac{1}{2}}_{\Phi\_}(f)\, \frac{\partial v_3}{\partial \Phi\_} \\ T(f) &< \frac{S^{\frac{1}{2}}_{\Phi\_}(f)\, \frac{\partial v_3}{\partial \Phi\_}}{S^{\frac{1}{2}}_{\phi\_}(f)\, \frac{\partial v_3}{\partial \phi\_}} \end{aligned} \tag{32}$$

To find a limit on $T(f)$ we substitute eq. (8) into eq. (32) and get

$$T(f) < \left(\frac{P_A}{P_S}\right)^{\frac{1}{2}} \left(\frac{\eta_S}{\eta_A}\right)^{\frac{1}{2}} \frac{\frac{\partial v_2}{\partial \phi\_}}{\frac{\partial v_3}{\partial \phi\_}}. \tag{33}$$

As we can see from Table 2, $\frac{\partial v_2}{\partial \phi\_} = \frac{\partial v_3}{\partial \phi\_}$. This is generally true of a non-recycled system as moving the beam splitter has equal and opposite effects on the light going to both ports. Therefore for a non-recycled system eq. (33) reduces to

$$T(f) < \left(\frac{P_A}{P_S}\right)^{\frac{1}{2}} \left(\frac{\eta_S}{\eta_A}\right)^{\frac{1}{2}}. \tag{34}$$

Thus $T(f > 100\ \text{Hz}) < 0.45$, or equivalently the open loop gain of the beam splitter control loop must satisfy

$$G(f > 100\ \text{Hz}) < 0.8. \tag{35}$$

As shown in Appendix A, the beam splitter control loop must also suppress low frequency seismic noise so that the residual motion is less than 4×10^{-9} m.

Martin Regehr has designed a loop shape for the LIGO beam splitter control which meets these requirements.[20] The open loop gain is shown in Figure 4. The seismic isolation in the 40-m lab is similiar in performance to the initial LIGO, but the ambient seismic noise is approximately ten times higher even during relatively seismically quiet times. Thus we use ten times the LIGO standard spectrum of test mass motion to estimate the motion in the 40-m interferometer. The residual motion after suppression by the beam splitter control system is shown in Figure 5. The residual RMS motion is 2.5×10^{-9} m.

Figure 4 Beam Splitter Loop Shape

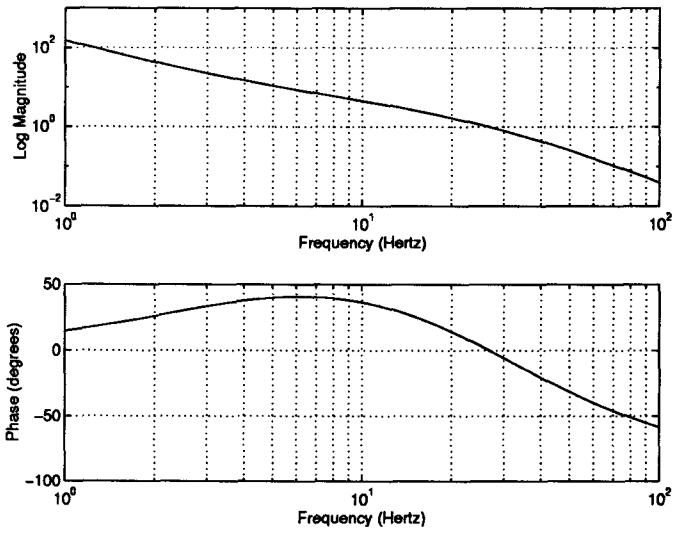

Figure 5 Residual Beam Splitter Motion

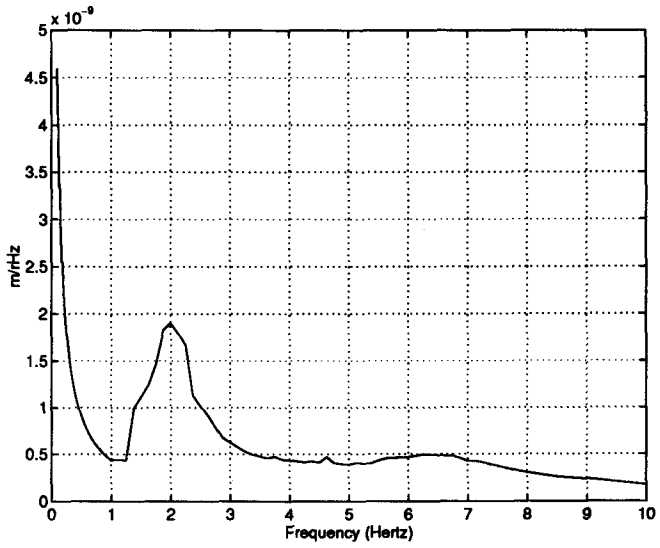

References

[1] D. Shoemaker, J. Giaime, F. Raab, M. Regehr, L. Sievers, "Comparison of 2 Fixed Mass Interferometer Testbeds and the Resulting Recommendation for the Initial LIGO Interferometer Design", Internal LIGO document (1993).

[2] S.E. Whitcomb, "Shot Noise in the Caltech Gravitational Wave Detector — The mid-1984 Configuration", with annotations by R.E. Spero, Internal LIGO document (1990).

[3] M. Regehr and T. Lyons, "Shot Noise in a Recycled Unbalanced LIGO", Internal LIGO document (1994).

[4] S. Kawamura, Intensity Noise Memo, dated June 24, 1992.

[5] 40-m Log Book #32, p. 98 white.

[6] 40-m Log Book #34, p. 59 white.

[7] M. Regehr, "Signal Extraction and Control for an Interferometric Gravitational Wave Detector", Appendix D, Caltech Ph.D. Thesis (1995). Note the loop 4 referred to in the thesis is the same as loop 2 here.

[8] M. Regehr, Table (5.2).

[9] R. Spero, private communication.

[10] D.Z. Anderson, "Alignment of resonant optical cavities", Applied Optics **23**, p. 2944–2949 (1984).

[11] M. Regehr, Appendix C.

[12] M. Regehr, equation (7.7).

[13] M. Regehr, equation (7.2).

[14] This appendix follows almost directly from M. Regehr, Appendix B.

[15] M. Regehr, equation (B.2).

[16] D. Shoemaker, "Considerations of the RMS motion of the LIGO cavity mirrors", LIGO Working Paper #109, Internal LIGO document (1992).

[17] D. Shoemaker, "Modulation and topology: Deviations from resonance", Internal LIGO document (1991).

[18] M. Regehr, equation (B.5).

[19] M. Regehr, equation (2.21).

[20] M. Regehr, Chapter 6.